nature photonics

LETTERS

PUBLISHED ONLINE: 29 APRIL 2012 | DOI: 10.1038/NPHOTON.2012.90

Speckle-free laser imaging using random laser illumination

Brandon Redding[1]*, Michael A. Choma[2,3]†* and Hui Cao[1,4]†*

Many imaging applications require increasingly bright illumination sources, motivating the replacement of conventional thermal light sources with bright light-emitting diodes, superluminescent diodes and lasers. Despite their brightness, lasers and superluminescent diodes are poorly suited for full-field imaging applications because their high spatial coherence leads to coherent artefacts such as speckle that corrupt image formation[1,2]. We recently demonstrated that random lasers can be engineered to provide low spatial coherence[3]. Here, we exploit the low spatial coherence of specifically designed random lasers to demonstrate speckle-free full-field imaging in the setting of intense optical scattering. We quantitatively show that images generated with random laser illumination exhibit superior quality than images generated with spatially coherent illumination. By providing intense laser illumination without the drawback of coherent artefacts, random lasers are well suited for a host of full-field imaging applications from full-field microscopy[4] to digital light projector systems[5].

Lasers are indispensable light sources in modern imaging systems. Intense laser sources enable imaging through scattering or absorptive media and allow dynamic behaviour to be measured on short timescales. One of the key properties of conventional lasers is high spatial coherence, a property that results from resonant cavities with a limited number of spatial modes that produce well-defined wavefronts. Such a high degree of spatial coherence has well-known advantages and disadvantages. On the one hand, high spatial coherence enables the highly directional emission of conventional lasers. However, spatial coherence also leads to coherent imaging artefacts, which originate from the interference that occurs during image formation. The resulting intensity modulations appear as additional features that are not present in the object, thereby corrupting the image. Coherent artefacts can be introduced, for example, by aberrations in an imaging system or simply by diffraction when imaging objects with sharp edges. However, the most common manifestation of coherent artefacts is speckle, which occurs when a rough object or scattering environment introduces random phase delays among mutually coherent photons that interfere at the detector[6]. Speckle is a long-standing issue because it impairs image interpretation by a human observer[7–9]. Over the years, various techniques have been developed to mitigate the effects of laser speckle by generating and averaging multiple uncorrelated speckle patterns (for instance, by scrambling the laser wavefront with a moving phase plate)[10]. However, for M independent speckle patterns, speckle contrast C is reduced as $M^{-1/2}$, fundamentally limiting the signal-to-noise ratio $(1/C)$ of a measurement to the number of speckle patterns generated (rather than the detector integration time or photon statistics)[2]. Accordingly, there is considerable interest in developing laser sources that fundamentally preclude the formation of coherent artefacts—in other words, a laser with low spatial coherence.

Random lasers are unconventional lasers in that they are made from disordered materials that trap light via multiple scattering[11,12]. The spatial modes are inhomogeneous and highly irregular. With external pumping, a large number of modes can lase simultaneously with uncorrelated phases. Their distinctly structured wavefronts combine to produce emission with low spatial coherence. Our recent studies have shown that the spatial coherence of random laser emission from a dye solution interspersed with scattering particles can be controlled by adjusting the scattering strength and pump geometry[3]. Based on this finding, we are able to engineer the random laser to achieve low spatial coherence. In this Letter, we demonstrate that a random laser with low spatial coherence can prevent the formation of speckle and produce high-quality images similar to those produced by conventional spatially incoherent sources such as light-emitting diodes (LEDs). We also present analysis indicating that random lasers can have a spectral radiance

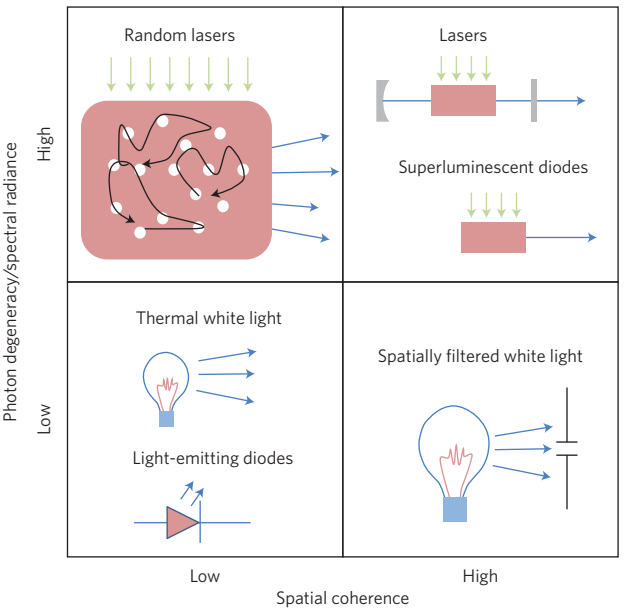

Figure 1 | Random lasers, a new kind of light source for imaging. Light sources are compared in terms of the two parameters most relevant to full-field imaging: photon degeneracy/spectral radiance and spatial coherence. Random lasers represent a new class of light source with high photon degeneracy/spectral radiance and low spatial coherence—the ideal combination for full-field imaging.

[1]Department of Applied Physics, Yale University, New Haven, Connecticut 06520, USA, [2]Departments of Diagnostic Radiology and of Pediatrics, Yale School of Medicine, New Haven, Connecticut 06520, USA, [3]Department of Biomedical Engineering, Yale University, New Haven, Connecticut 06520, USA, [4]Department of Physics, Yale University, New Haven, Connecticut 06520, USA; †These authors contributed equally to the work.
*e-mail: brandon.redding@yale.edu; michael.choma@yale.edu; hui.cao@yale.edu

© 2012 Macmillan Publishers Limited. All rights reserved.

and photon degeneracy superior to LEDs and comparable to superluminescent diodes (SLDs) and broadband lasers.

Imaging without coherent artefacts requires illumination of a sample with a large number of mutually incoherent photons. The number of photons per coherence volume (that is, the photon degeneracy parameter δ) is therefore a relevant measure of source power because photons from distinct coherence volumes cannot interfere to generate coherent artefacts. From this perspective, the limitations of thermal sources and conventional lasers are clear. On the one hand, thermal sources (lower left quadrant in Fig. 1) generate coherent artefact-free images (low spatial coherence), but have very few photons per coherence volume (low photon degeneracy). On the other hand, conventional lasers (upper right quadrant in Fig. 1) have many photons per coherence volume (high photon degeneracy) but readily generate coherent artefacts (high spatial coherence). There is therefore a need for sources with high photon degeneracy and low spatial coherence, a need that can be filled by random lasers (upper left quadrant in Fig. 1).

We estimated the photon degeneracy parameter of our random lasers for comparison with existing light sources. Note that the photon degeneracy parameter δ is directly proportional to the spectral radiance, a radiometric measure of the amount of radiation through a unit area and into a unit solid angle within a unit frequency bandwidth[13]. For a thermal source, δ depends on the temperature and is $\sim 1 \times 10^{-3}$ at 4,000 K (ref. 13). A high-efficiency LED has δ on the order of 1×10^{-2} (ref. 14). SLDs and broadband lasers, both exhibiting high spatial coherence, have a photon degeneracy much larger than 1. For a typical SLD, δ is estimated to be $\sim 1 \times 10^{3}$ (ref. 15), whereas a pulsed Ti:sapphire laser has $\delta \approx 1 \times 10^{6}$. Narrowband lasers not only exhibit high spatial coherence, but also have long temporal coherence, leading to extremely high photon degeneracy. For example, a typical HeNe laser emitting 1 mW has a δ of $\sim 1 \times 10^{9}$ (ref. 13). Random lasers with low spatial and temporal coherence have smaller δ. For the dye random laser used in this work, the low repetition rate of our pump laser (10 Hz) further reduces δ to $\sim 1 \times 10^{-2}$. However, conventional dye lasers routinely operate at repetition rates of ~100 MHz (refs 16–19). We performed experiments demonstrating that the average pump power and pulse spacing required for operation at a 1 MHz repetition rate did not adversely affect the random laser performance (see Supplementary Information), and we therefore expect that our random laser system can be scaled up to approximately megahertz repetition rates, producing a δ of $\sim 1 \times 10^{3}$. This level of photon degeneracy would provide several orders of magnitude improvement over existing spatially incoherent sources. As illustrated in Fig. 1, this combination of high photon degeneracy and low spatial coherence has not been realized in other light sources and makes random lasers uniquely suited for imaging applications.

To demonstrate that a low-spatial-coherence random laser does in fact enable speckle-free imaging, we compared images generated with random laser illumination to those generated by other common light sources: a narrowband laser, a broadband laser and an LED. We also considered an amplified spontaneous emission (ASE) source generated from the same dye solution as the random laser, only without the scattering particles. The ASE source has a higher spatial coherence than the random laser, but produces a similar emission spectrum[3], and it is qualitatively similar to a SLD. Additional information regarding these sources can be found in the Supplementary Information. Our imaging tests were conducted in transmission mode using Köhler illumination. Images were formed using a single, aberration-corrected finite conjugate ×10 objective. A Young's double slit experiment was conducted to characterize the spatial coherence of the sources on the object plane. The narrowband laser and the broadband laser exhibited the highest spatial coherence, followed by the ASE source. The random laser had significantly lower spatial coherence, and the LED

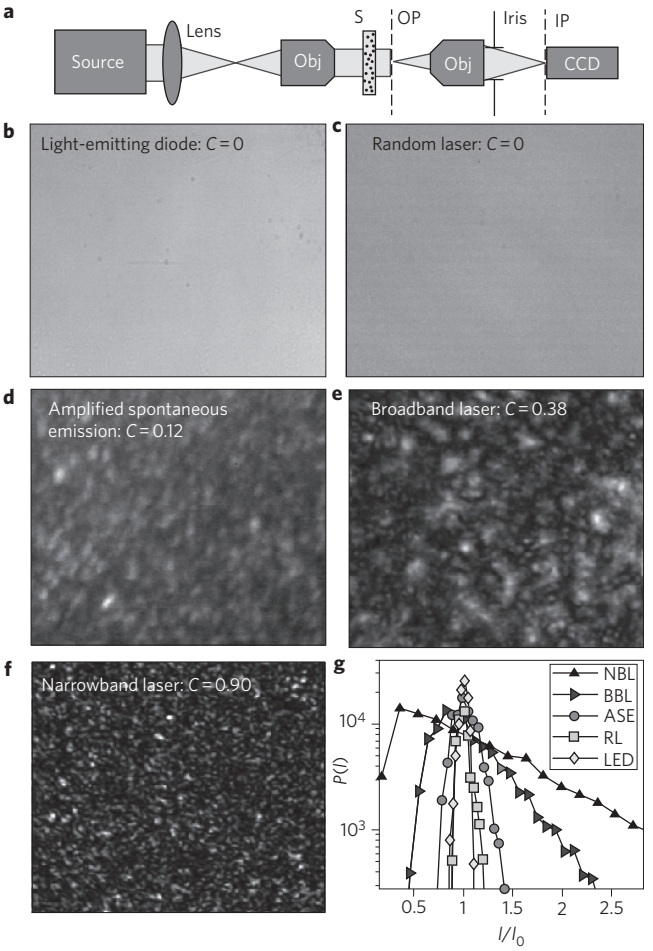

Figure 2 | Random lasers prevent speckle formation. a, Schematic of experimental set-up. Five light sources with different degrees of spatial coherence were used: a light-emitting diode (LED), a random laser (RL), an amplified spontaneous emission (ASE) source, a broadband laser (BBL) and a narrowband laser (NBL). These illuminated a scattering film and imaged the transmitted signal onto a CCD camera. Obj, microscope objective; S, scattering film; OP, object plane; IP, image plane. **b–f**, Speckle contrast C decreases with spatial coherence of the source. The random laser effectively prevents speckle formation, behaving similarly to the LED but very differently from conventional lasers. **g**, Intensity fluctuations in the images are measured by the probability density function of light intensity (I) at each pixel of the camera, normalized by the average intensity (I_0), of all pixels. The distribution becomes narrower as the spatial coherence reduces.

the lowest. Further experimental details are contained in the Supplementary Information.

We first show that the random laser can prevent speckle formation. In this experiment, there is no imaging object on the object plane, and light from the source passes through a scattering film (Fig. 2a). Images taken with the five illumination sources are presented in Fig. 2b–f. Speckle is clearly visible when using the narrowband laser, broadband laser and ASE source, but the images collected using the random laser and the LED do not exhibit any measurable speckle. As a quantitative comparison, we extracted the probability P of finding a pixel with a given intensity I, normalized by the average intensity I_0, from all the pixels. This probability density function is plotted in Fig. 2g. The relatively narrow intensity distribution for the random laser and LED illumination contrasts with the increasingly broad distributions produced by the ASE, broadband laser and narrowband laser. We also extracted the speckle contrast ($C = \sigma_I / \langle I \rangle$, where σ_I is the standard deviation

© 2012 Macmillan Publishers Limited. All rights reserved.

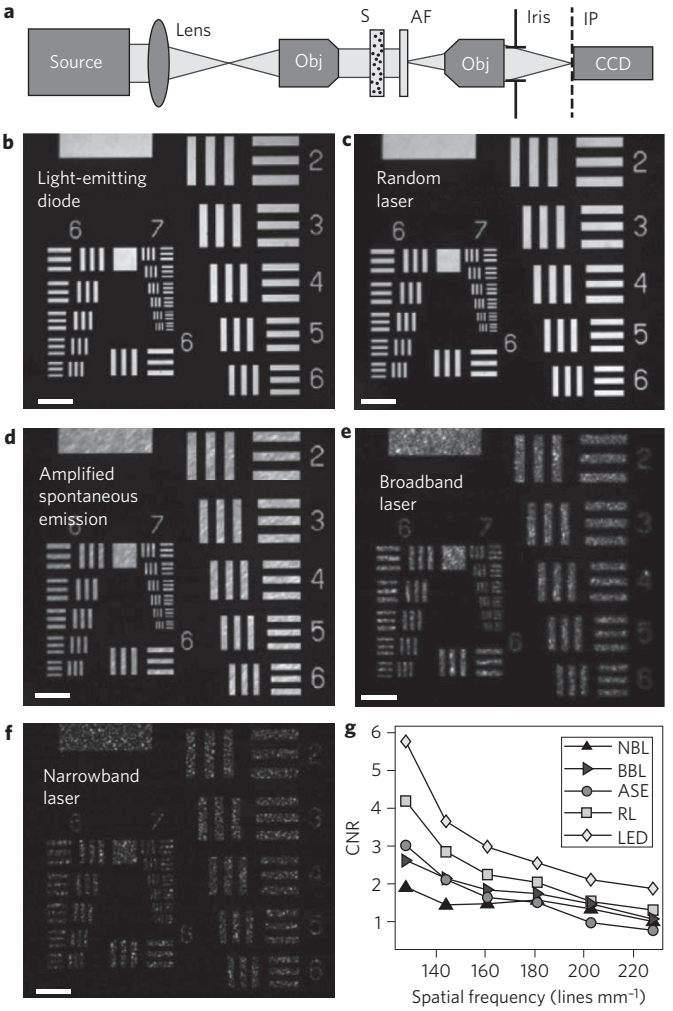

Figure 3 | Random lasers produce speckle-free images. a, Schematic of the experimental set-up. We used five light sources, described in Fig. 2, to image an AF resolution test chart. A scattering film was placed in front of the object, which resulted in speckled illumination of the object if the source was spatially coherent. Obj, microscope objective; S, scattering film; AF, AF test chart; IP, image plane. **b–f**, Images taken with the five sources showing that the spatially coherent sources, particularly the narrowband laser and the broadband laser, produce speckles in the bright area of the image (transparent bars in the test chart). The background of the image, which corresponds to the opaque area on the object, remains dark. Scale bars, 50 μm. **g**, As a quantitative measure of image degradation by the speckle, the CNR was extracted from the images and plotted as a function of the spatial frequency of the features on the test chart. This confirms that the random laser produces superior images to conventional lasers and the ASE source.

of the intensity and $\langle I \rangle$ is the average intensity) from each image and found that it increased with the degree of spatial coherence of the source.

We then demonstrate that the ability of a random laser to prevent speckle formation translates to improved image quality. A 1951 US Air Force (AF) resolution test chart was imaged with the same five light sources. The scattering film was placed on the illumination side of the AF chart (Fig. 3a) to impart random phase delays to the incident light, which resulted in speckled illumination of the object if the source had a high degree of spatial coherence. This configuration is also equivalent to imaging an optically rough object[2]. Images collected with the five sources are presented in Fig. 3b–f. The spatially coherent sources, particularly the narrowband laser and the broadband laser, exhibit speckle patterns within the bars of the AF chart. These artificial intensity modulations, which have no relationship with the features on the AF chart, corrupt the image. The low-spatial-coherence random laser and LED, however, eliminate interference effects and produce a clean image of the object. Image quality can be compared quantitatively using the contrast-to-noise ratio (CNR), which is defined as $(\langle I_f \rangle - \langle I_b \rangle)/((\sigma_f + \sigma_b)/2)$, where $\langle I_f \rangle$ is the average intensity of the feature of interest (for example, a bar in the AF test chart), $\langle I_b \rangle$ is the average intensity of the surrounding background, and σ is the standard deviation of pixel intensity. The CNR describes the identifiability of a feature of interest in a given background[20]. As shown in Fig. 3g, the CNR decreases with increasing spatial coherence. When the CNR approaches unity, feature contrast is comparable to image noise. Hence, speckle dramatically degrades image quality at high spatial coherence.

The benefits of using a low-spatial-coherence random laser are even more pronounced when imaging is performed in a scattering environment. To investigate this, we imaged the AF test chart through the scattering film (Fig. 4a). Images collected with the five sources are shown in Fig. 4b–f. In comparison with the images in Fig. 3b–f, the scattering film can be seen to have effectively increased the background signal, because scattered photons were mis-mapped to what would otherwise be dark background regions of the image, that is, regions that correspond to opaque portions of the AF test chart. Under spatially coherent illumination, interference among these scattered photons (crosstalk) resulted in speckle that corrupted the image beyond recognition. However, when illuminating with a low-spatial-coherence source, interference among scattered photons was precluded, leading to a uniform background signal. As a result, although the scattering medium decreased the image contrast, the features of the object remained visible. Again, we estimated the CNR for each image, as shown in Fig. 4g. The CNRs for the conventional lasers and ASE source are below unity, consistent with our qualitative assessment that these images contain few to no interpretable features. Only the random laser and the LED were able to produce CNRs greater than unity, corresponding to recognizable images. Therefore, the random laser can eliminate the crosstalk that produces speckle.

The above experiments illustrate that random lasers are ideally suited for imaging in scattering environments, a common situation in biological imaging or imaging through atmospheric turbulence. The high degree of scattering in these environments not only introduces intense crosstalk, requiring a source with low spatial coherence, but also causes loss, requiring a source with brighter illumination than can be achieved with existing spatially incoherent sources. By meeting these two requirements, random laser sources can enable parallel (full-field) imaging in scattering environments. Furthermore, the unique ability of random lasers to provide tunable spatial coherence opens the possibility of optimizing the illumination source for a specific imaging application. The degree of spatial incoherence required to prevent speckle formation depends on the parameters of a specific imaging application (for example, imaging numerical aperture, sample roughness[21–23]). As such, a random laser could be designed to provide sufficiently low spatial coherence to eliminate speckle while maintaining a high photon degeneracy relative to existing spatially incoherent sources.

In conclusion, we have demonstrated that random lasers are a new kind of light source that is ideal for full-field imaging. Because they generate stimulated emission in many different spatial modes, random lasers exhibit a laser-level intensity with low spatial coherence, two properties that have traditionally been mutually exclusive in light sources (for example, thermal sources, LEDs or conventional lasers). Over the past decade, random lasers have been realized in a wide range of material systems, including solid-state and semiconductor-based systems with emission

© 2012 Macmillan Publishers Limited. All rights reserved.

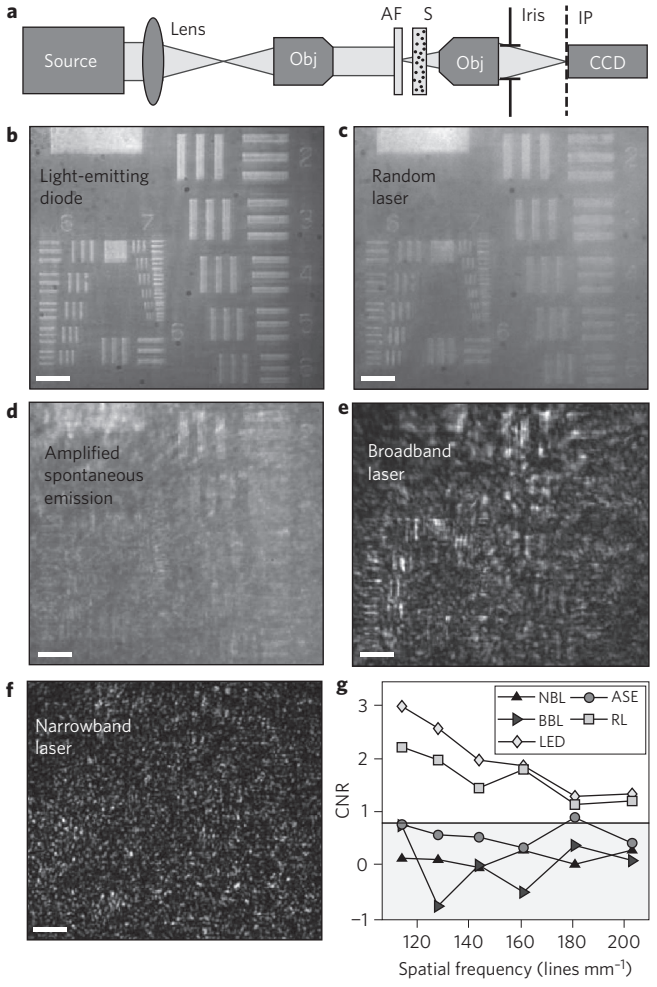

Figure 4 | Random lasers prevent crosstalk during image formation. a, Schematic of the experimental set-up. We used five light sources, described in Fig. 2, to image an AF resolution test chart through a scattering film that was positioned on the detection side of the object. Obj, microscope objective; S, scattering film; AF, AF test chart; IP, image plane. **b–f**, Images taken with the five sources. Scale bars, 50 μm. Under spatially coherent illumination, speckle is produced everywhere across the image and very little information about the object is detected. However, the low spatial coherence of the random laser and the LED eliminate speckle, and the scattering merely increases the background level uniformly, so the features of the object are still visible. **g**, As a quantitative measure of image quality, the CNR was extracted from the images and plotted versus the spatial frequency of the features on the test chart. Only the random laser and the LED can produce images with CNR values greater than unity.

frequencies ranging from the ultraviolet to the near-infrared. They can be pumped either optically[24] or electrically[25,26]. We anticipate that these systems could also provide low spatial coherence based on similar design principles[3] and could therefore be used for speckle-free imaging. Some of these random lasers operate at a high repetition rate (82 MHz)[27], or even continuously in time[28,29], which would facilitate the achievement of high photon degeneracy. In addition to low spatial coherence, random lasers can exhibit low temporal coherence. The temporal coherence length of the dye random laser used in this work, for instance, can be estimated from the emission bandwidth to be ∼17 μm (ref. 30). This short temporal coherence would allow random lasers to be used in coherent imaging applications such as optical coherence tomography[31,32], which is also known to suffer from spatial-coherence-induced artefacts[33,34]. The versatility of random laser systems, combined with their controllable coherence and laser-level intensity, could lead to their use in a wide range of imaging applications.

Methods

Our random laser system was composed of colloidal solutions of polystyrene spheres and laser dye Rhodamine 640 (5 mmol), which was dissolved in diethylene glycol. The polystyrene spheres were ∼240 nm in diameter, and their scattering cross-section was calculated to be 1.67×10^{-11} cm^2. The sphere concentration was 6.1×10^{12} cm^{-3}, yielding a scattering mean free path of ∼100 μm. The ASE source was obtained from the same dye solution (5 mmol Rhodamine 640) without polystyrene spheres. Both solutions were stored in a 1 cm × 1 cm cuvette and optically excited by a frequency-doubled Nd:YAG laser ($\lambda = 532$ nm) with 30 ps pulses at a repetition rate of 10 Hz. The pump beam was focused to a ∼300-μm-diameter spot on the front window of the cuvette. Emission from the solutions was separated from the pump beam with a dichroic mirror and then directed to the imaging experiment set-up. The narrowband laser source used in this work was a HeNe gas laser operating at $\lambda = 633$ nm. The broadband laser light was generated by a mode-locked Ti:sapphire laser with 200 fs pulses at a repetition rate of 76 MHz. The Ti:sapphire pulses at $\lambda \approx 790$ nm produced a supercontinuum in a photonic-crystal fibre and the visible component centred at ∼640 nm with a bandwidth of ∼40 nm was used as a broadband coherent light source. The LED used in this work was a SugarCube Red LED with a centre wavelength of ∼630 nm and a bandwidth of 15 nm. The emission spectra of all five sources are presented in the Supplementary Information.

The scattering films used in the imaging experiments consisted of TiO_2 particles spun onto glass substrates. The particles were ∼20 nm in diameter and the transport mean free path was ∼600 nm. The amount of scattering was controlled by the film thickness, which was 3 μm for the experiments in Figs 2–4.

Finite conjugate microscope object lenses (Newport M-Series) were used in the imaging experiments. The images in Figs 2–4 were collected with a ×10 objective lens with a numerical aperture of 0.25 and a cooled COHU 4920 monochrome CCD.

Received 6 March 2011; accepted 25 March 2012; published online 29 April 2012

References

1. Oliver, B. M. Sparkling spots and random diffraction. *Proc. IEEE* **51,** 220–221 (1963).
2. Goodman, J. W. Optical methods for suppressing speckle, in *Speckle Phenomena in Optics* 141–186 (Roberts & Company, 2007).
3. Redding, B., Choma, M. A. & Cao, H. Spatial coherence of random laser emission. *Opt. Lett* **36,** 3404–3406 (2011).
4. Dingel, B. & Kawata, S. Speckle-free image in a laser-diode microscope by using the optical feedback effect. *Opt. Lett.* **18,** 549–551 (1993).
5. Yurlov, V., Lapchuk, A., Yun, S., Song, J. & Yang, H. Speckle suppression in scanning laser display. *Appl. Opt.* **47,** 179–187 (2008).
6. Rigden, J. D. & Gordon, E. I. The granularity of scattered optical maser light. *Proc. Inst. Radio Eng.* **50,** 2367–2368 (1962).
7. Geri, A. G. & Williams, L. A. Perceptual assessment of laser-speckle contrast. *J. Soc. Inf. Displ.* **20,** 22–27 (2012).
8. Gaska, J. P., Tai, C. & Geri, G. A. Laser-speckle properties and their effect on target detection *J. Soc. Inf. Displ.* **15,** 1023–1028 (2007).
9. Artigas, J. M., Felipe, A. & Buades, M. J. Contrast sensitivity of the visual system in speckle imagery. *J. Opt. Soc. Am. A* **11,** 2345–2349 (1994).
10. McKechnie, T. S. Speckle reduction, in *Topics in Applied Physics* Vol. 9 (ed. Dainty, J. C.) 123–170 (Springer, 1975).
11. Cao, H. Lasing in disordered media, in *Progress in Optics* Vol. 45 (ed. Wolf, E.) 317–370 (North-Holland, 2003).
12. Wierma, D. S. The physics and applications of random lasers. *Nature Phys.* **4,** 359–367 (2008).
13. Mandel, L. & Wolf, E. *Optical Coherence and Quantum Optics* (Cambridge Univ. Press, 1995).
14. SugarCUBE^{TM} Red, Nathaniel Group, Vergennes, VT, USA; available at http://www.nathaniel.com/sugarcube.php
15. Hitzenberger, C. K., Danner, M., Drexler, W. & Fercher, A. F. Measurement of the spatial coherence of superluminescent diodes. *J. Mod. Opt.* **46,** 1763–1774 (1999).
16. Chesnoy, J. & Fini, L. Stabilization of a femtosecond dye laser synchronously pumped by a frequency-doubled mode-locked YAG laser. *Opt. Lett.* **11,** 635–637 (1986).
17. Knox, W. H. & Beisser, F. A. Two-wavelength synchronous generation of femtosecond pulses with 100-fs jitter. *Opt. Lett.* **17,** 1012–1014 (1992).
18. Johnson, A. M. & Simpson, W. M. Continuous-wave mode-locked Nd:YAG-pumped subpicosecond dye lasers. *Opt. Lett.* **8,** 554–556 (1983).
19. Seifert, F. & Petrov, V. Synchronous pumping of a visible dye laser by a frequency double mode-locked Ti:sapphire laser and its application for difference frequency generation in the near infrared. *Opt. Commun.* **99,** 413–420 (1993).
20. Bryan, R. N. *Introduction to the Science of Medical Imaging* (Cambridge Univ. Press, 2009).

© 2012 Macmillan Publishers Limited. All rights reserved.

21. Kang, D. & Milster, T. D. Simulation method for non-Gaussian speckle in a partially coherent system. *J. Opt. Soc. Am. A* **26,** 1954–1960 (2009).
22. Kang, D. & Milster, T. D. Effect of optical aberration on Gaussian speckle in a partially coherent imaging system. *J. Opt. Soc. Am. A* **26,** 2577–2585 (2009).
23. Kang, D. & Milster, T. D. Effect of fractal rough-surface Hurst exponent on speckle in imaging systems. *Opt. Lett.* **34,** 3247–3249 (2009).
24. Cao, H. *et al.* Random laser action in semiconductor powder. *Phys. Rev. Lett.* **82,** 2278–2281 (1999).
25. Leong, E. S. P. & Yu, S. F. UV random lasing action in p-SiC(4H)/i-ZnO-SiO_2 nanocomposite/n-ZnO:Al heterojunction diodes. *Adv. Mater.* **18,** 1685–1688 (2006).
26. Zhu, H. *et al.* Low-threshold electrically pumped random lasers. *Adv. Mater.* **22,** 1877–1881 (2010).
27. Xu, J. & Xiao, M. Lasing action in colloidal CdS/CdSe/CdS quantum wells. *Appl. Phys. Lett.* **87,** 173117 (2005).
28. Chu, S., Olmedo, M., Yang, Z., Kong, J. & Liu, J. Electrically pumped ultraviolet ZnO diode lasers on Si. *Appl. Phys. Lett.* **93,** 181106 (2008).
29. Ma, X., Chen, P., Li, D., Zhang, Y. & Yang, D. Electrically pumped ZnO film ultraviolet random lasers on silicon substrate. *Appl. Phys. Lett.* **91,** 251109 (2007).
30. Papadakis, V. M. *et al.* Single-shot temporal coherence measurements of random lasing media. *J. Opt. Soc. Am. B* **24,** 31–36 (2007).
31. Redding, B., Choma, M. A. & Cao, H. Spatially incoherent random lasers for full field optical coherence tomography, in *Conference on Lasers and Electro-Optics*, PDPC7 (Optical Society of America, 2011).
32. Huang, D. *et al.* Optical coherence tomography. *Science* **254,** 1178–1181 (1991).
33. Karamata, B. *et al.* Multiple scattering in optical coherence tomography. I. Investigation and modeling. *J. Opt. Soc. Am. A* **22,** 1369–1379 (2005).
34. Karamata, B. *et al.* Multiple scattering in optical coherence tomography. II. Experimental and theoretical investigation of cross talk in wide-field optical coherence tomography. *J. Opt. Soc. Am. A* **22,** 1380–1388 (2005).

Acknowledgements

H.C. acknowledges support from the National Science Foundation (grants ECCS-1128542 and ECCS-1068642). M.A.C. acknowledges support through a K12 award from the Yale Child Health Research Center (5K12-HD001401-12). The authors wish to thank A.D. Stone, E.R. Dufresne, L.H. Staib and H.D. Tagare for discussions and H. Noh for technical assistance.

Author contributions

M.A.C and H.C. initiated the study. B.R. set up the experiments and collected all the data in the laboratory of H.C. B.R. analysed the data and prepared the manuscript. M.A.C. and H.C. contributed extensively to data interpretation and manuscript preparation.

Additional information

The authors declare competing financial interests: details accompany the full-text HTML version of the paper at www.nature.com/naturephotonics. Supplementary information accompanies this paper at www.nature.com/naturephotonics. Reprints and permission information is available online at http://www.nature.com/reprints. Correspondence and requests for materials should be addressed to B.R., M.A.C. and H.C.

© 2012 Macmillan Publishers Limited. All rights reserved.